coring and also would be candidate horizons of the Tohoku-Oki rupture.

The fault zone at the drill site is thinner with more penetrative scaly fabric and with less extensive deformation in adjacent sediments than fault zones observed in previous ocean-drilling and onland studies (*18*, *19*). Accommodation of kilometers of shear displacement in the <5-m-thick scaly clay demonstrates marked long-term slip localization and that the clay layer has been weak relative to the bounding mudstones over the duration of fault activity (*16*, *20*). Indeed, the layer must be weaker than the surrounding sediments during periods of both seismic slip and interseismic creep. This finding is corroborated by direct laboratory measures of sliding friction for samples of the scaly clay at high shear rates (*21*) and of similar clay-rich materials at low shear rates (*22*).

Large slip during most historical earthquakes in the northwest Pacific did not extend close to the trench, but, when it has, there have been devastating consequences from unusually large tsunamis [the 1896 Meiji-Sanriku and 2011 Tohoku-Oki earthquakes (*23*, *24*)]. Similar to the shallow slip zone of the 2011 Tohoku-Oki earthquake, some other subduction zones show evidence that the lithostratigraphy of the incoming plate influences the location and the architecture of the plate-boundary fault [e.g., Barbados (*25*) and Sumatra (*26*)]. The pelagic sediments below the plate-boundary fault at the JFAST drill site are similar to those over much of the northwestern Pacific Plate (*27*). Because the site shares a history and stratigraphy with the rest of the northern Japan Trench, it is possible that the structure and relative mechanical properties observed here may be representative of the subduction thrusts throughout the region.

References and Notes

1. A. Hasegawa, K. Yoshida, T. Okada, *Earth Planets Space* **63**, 703–707 (2011).
2. A. Kato, S. Sakai, K. Obara, *Earth Planets Space* **63**, 745–748 (2011).
3. W. Lin *et al.*, *Science* **339**, 687–690 (2013).
4. T. Fujiwara *et al.*, *Science* **334**, 1240 (2011).
5. Y. Ito *et al.*, *Geophys. Res. Lett.* **38**, L00G05 (2011).
6. Y. Fujii, K. Satake, S. Sakai, M. Shinohara, T. Kanazawa, *Earth Planets Space* **63**, 815–820 (2011).
7. F. M. Chester, J. J. Mori, N. Eguchi, S. Toczko, Expedition 343/343T Scientists, *Proc. IODP*, **343/343T** (2013); available online at http://publications.iodp.org/proceedings/343_343T/343title.htm.
8. C. J. Ammon, T. Lay, H. Kanamori, M. Cleveland, *Earth Planets Space* **63**, 693–696 (2011).
9. K. D. Koper, A. R. Hutko, T. Lay, C. J. Ammon, H. Kanamori, *Earth Planets Space* **63**, 599–602 (2011).
10. S. Kodaira *et al.*, *Nat. Geosci.* **5**, 646–650 (2012).
11. Y. Nakamura, S. Kodaira, S. Miura, C. Regalla, N. Takahashi, *Geophys. Res. Lett.* **40**, 1713–1718 (2013).
12. T. Tsuru *et al.*, *J. Geophys. Res. Solid Earth* **107**, 2357 (2002).
13. P. M. Fulton *et al.*, *Science* **342**, 1214–1217 (2013).
14. Shipboard Scientific Party, *Init. Rep. DSDP* **56 and 57** (Part 1), 399–446 (1980); available online at www.deepseadrilling.org/56_57/volume/dsdp56_57pt1_07.pdf.
15. P. Vannucchi, A. Maltman, G. Bettelli, B. Clennell, *J. Struct. Geol.* **25**, 673–688 (2003).
16. F. M. Chester, J. S. Chester, *Tectonophysics* **295**, 199–221 (1998).
17. A. M. Lin, Z. K. Ren, Y. Kumahara, *J. Struct. Geol.* **32**, 781–791 (2010).
18. C. D. Rowe, J. C. Moore, F. Remitti, IODP Expedition 343/343T Scientists, *Geology* **41**, 991–994 (2013).
19. H. M. Savage, E. E. Brodsky, *J. Geophys. Res.* **116**, B03405 (2011).
20. R. H. Sibson, *Bull. Seismol. Soc. Am.* **93**, 1169–1178 (2003).
21. K. Ujiie *et al.*, *Science* **342**, 1211–1214 (2013).
22. D. A. Lockner, C. Morrow, D. Moore, S. Hickman, *Nature* **472**, 82–85 (2011).
23. Y. Tanioka, K. Satake, *Geophys. Res. Lett.* **23**, 1549–1552 (1996).
24. T. Lay *et al.*, *J. Geophys. Res. Solid Earth* **117**, B04311 (2012).
25. G. Wallace, J. C. Moore, C. G. DiLeonardo, *Geol. Soc. Am. Bull.* **115**, 288–297 (2003).
26. S. M. Dean *et al.*, *Science* **329**, 207–210 (2010).
27. D. R. Horn, B. M. Horn, M. N. Delach, *Geol. Soc. Am.* **126**, 1–22 (1970).
28. C. DeMets, R. G. Gordon, D. F. Argus, *Geophys. J. Int.* **181**, 1–80 (2010).
29. Materials and methods are available as supplementary materials on *Science* Online.

Acknowledgments: This research used samples and data provided by the IODP (www.iodp.org/access-data-and-samples). We thank all drilling and logging operation staff on board the D/V *Chikyu* during expedition 343 and 343T. Part of this work was supported by the U.S. Science Support Program of IODP, and participation by E.B. was funded in part by the Gordon and Betty Moore Foundation. F.M.C., C. Rowe, K.U., C. Regalla, J. Kirkpatrick, F.R., J.C.M., and E.E.B. prepared figures and wrote the manuscript; C. Regalla, J. Kirkpatrick, F.R., V.T., M.W.-S., S.B., and J. Kameda provided structural and lithologic descriptions of core samples; J.J.M., E.E.B., S. Kodaira, F.M.C., P. Fulton, N.E., and S.T. organized and managed the expedition; all expedition scientists contributed to the paper by providing shipboard measurements and scientific discussions.

Supplementary Materials

www.sciencemag.org/content/342/6163/1208/suppl/DC1
Materials and Methods
Supplementary Text
Figs. S1 to S3
References

24 July 2013; accepted 30 October 2013
10.1126/science.1243719

Low Coseismic Shear Stress on the Tohoku-Oki Megathrust Determined from Laboratory Experiments

Kohtaro Ujiie,[1,2]* Hanae Tanaka,[1] Tsubasa Saito,[1] Akito Tsutsumi,[3] James J. Mori,[4] Jun Kameda,[5] Emily E. Brodsky,[6] Frederick M. Chester,[7] Nobuhisa Eguchi,[8] Sean Toczko,[8] Expedition 343 and 343T Scientists†

Large coseismic slip was thought to be unlikely to occur on the shallow portions of plate-boundary thrusts, but the 11 March 2011 Tohoku-Oki earthquake [moment magnitude (M_w) = 9.0] produced huge displacements of ~50 meters near the Japan Trench with a resultant devastating tsunami. To investigate the mechanisms of the very large fault movements, we conducted high-velocity (1.3 meters per second) friction experiments on samples retrieved from the plate-boundary thrust associated with the earthquake. The results show a small stress drop with very low peak and steady-state shear stress. The very low shear stress can be attributed to the abundance of weak clay (smectite) and thermal pressurization effects, which can facilitate fault slip. This behavior provides an explanation for the huge shallow slip that occurred during the earthquake.

Megathrust earthquakes commonly occur in subduction zones at depths where there is strong locking between the plates and long-term strain accumulation (*1*, *2*). In general, unconsolidated, soft sediments in the shallow region of the plate-boundary thrust (décollement) were thought to slip aseismically and have low levels of locking (*3*). The widely accepted view was that rupture during large earthquakes was unlikely to produce large slip on the shallow décollement (*1*–*3*). However, the coseismic fault slip extended all the way to the trench axis during the 11 March 2011 Tohoku-Oki earthquake [moment magnitude (M_w) = 9.0] with very large slip (~50 m), resulting in the huge tsunami that devastated much of the east coast of northern Honshu, Japan (*4*–*8*).

The Integrated Ocean Drilling Program (IODP) Expedition 343 and 343T, Japan Trench Fast Drilling Project (JFAST), provided an invaluable opportunity to investigate the plate-boundary décollement near the Japan Trench (*9*). JFAST successfully drilled the décollement at ~820 m

[1]Graduate School of Life and Environmental Sciences, University of Tsukuba, Tsukuba, Japan. [2]Institute for Research on Earth Evolution, Japan Agency for Marine-Earth Science and Technology, Yokosuka, Japan. [3]Graduate School of Science, Kyoto University, Kyoto, Japan. [4]Disaster Prevention Research Institute, Kyoto University, Kyoto, Japan. [5]Department of Natural History Sciences, Hokkaido University, Sapporo, Japan. [6]Department of Earth and Planetary Sciences, University of California Santa Cruz, Santa Cruz, CA 95060, USA. [7]Center for Tectonophysics, Department of Geology and Geophysics, Texas A&M University, College Station, TX 77843–3115, USA. [8]Center for Deep Earth Exploration, Japan Agency for Marine-Earth Science and Technology, Yokohama, Japan.

*Corresponding author. E-mail: kujiie@geol.tsukuba.ac.jp
†Expedition 343 and 343T Scientists authors and affiliations are listed in the supplementary materials.

below the sea floor (mbsf) in water depths of ~6900 m at site C0019, located at the toe of the frontal prism in the area of large shallow slip during the 2011 earthquake. The décollement mostly consists of highly sheared clays that are marked by polished and striated surfaces wrapping around more intact lenses. The sheared clays are red-brown and dark brown to black in color and are similar to pelagic clays deposited on the incoming Pacific Plate (*10*, *11*). Summing the unrecovered intervals with the actual core recovery of highly deformed material constrains the total thickness of the décollement interval to be less than 4.86 m. The total thickness of the décollement-related damage zone is ≤10 m, including both overlying frontal prism material and underlying subducted sediments. The drilling results at site C0019 clarified that plate-boundary faulting in this region is highly localized in pelagic clay (*10*).

To determine frictional properties that control the earthquake slip, we used a rotary shear apparatus capable of high velocity and large slip to conduct laboratory tests on the décollement material taken from site C0019 (*12*). The recovered décollement material may not include the principal slip surface of the Tohoku-Oki earthquake, but it is the host material of the earthquake slip zone, and therefore studying its frictional behavior at high slip rates helps us understand the obersved large coseismic slip. Experimental parameters were set at an equivalent slip rate of 1.3 m s^{-1}, normal stresses of ~2.0 MPa, and displacements of ~15 to 60 m, which are comparable to the conditions of fault slip during the earthquake. We also simulated permeable and impermeable conditions during high-velocity shearing because permeability is an important factor in controlling frictional behavior. The actual fault conditions during the earthquake could be partially drained and thus lie between these two end-member cases.

The measurements of shear stress at a normal stress of 2.0 MPa showed an initial peak during slip of less than 1-m displacement, then quickly dropped to steady-state values of ~0.4 and ~0.2 MPa for the permeable and impermeable cases, respectively (Fig. 1, A and B). Compared with the permeable tests, the impermeable tests show lower values of shear stress (Fig. 1C) (*12*). For the same amount of displacement, the calculated temperature in the gouge is always smaller for the impermeable tests compared with the permeable tests, likely because thermal expansion of pore fluids raises the local fluid pressure in the sheared gouge and thus decreases the effective normal stress. The axial displacement data indicate that the section of rock specimen-gouge compacted and then dilated for both the permeable and impermeable tests. There is more compaction in the permeable tests relative to the impermeable tests, consistent with an easier escape of water from the gouge to the specimen (permeable Berea sandstone). The initial compaction during impermeable tests may be due to the development of foliated zones in the gouge (Fig. 2C). For permeable tests, the dilation occurs in association with the thermal expansion of quartz grains in the sandstone that is noteworthy at temperatures of 500° to 573°C (*13*). For the impermeable tests, thermal expansion of quartz grains is unlikely to occur because of the smaller temperature rise in the gouge and a smaller fraction of quartz in the specimen (Indian gabbro); therefore, the dilation is attributed to thermal expansion of pore fluid in the gouge material itself. These experimental results indicate that for impermeable conditions, the gouge material of the shallow décollement can be weakened due to effective thermal pressurization (*14*–*16*).

For permeable tests, there is a dependence of shear stress on normal stress (Fig. 1C). For the impermeable tests, the shear stress at the peak and steady state is weakly dependent and independent of normal stress, respectively. We extrapolate the relations between the steady-state shear stress and normal stress under permeable and impermeable cases (equations in Fig. 1C) to the effective normal stress at a depth of 820 mbsf on the décollement at site C0019 (7 MPa) (*17*). This yields values of shear stress for the in situ condition under permeable and impermeable cases of 1.32 and 0.22 MPa, respectively, which correspond to values for the in situ apparent coefficient of friction under permeable and impermeable conditions of 0.19 and 0.03, respectively. JFAST installed temperature sensors across the fault zone to estimate the frictional heat associated with the huge shallow slip during the 2011 Tohoku-Oki earthquake. The slip-averaged shear stress and

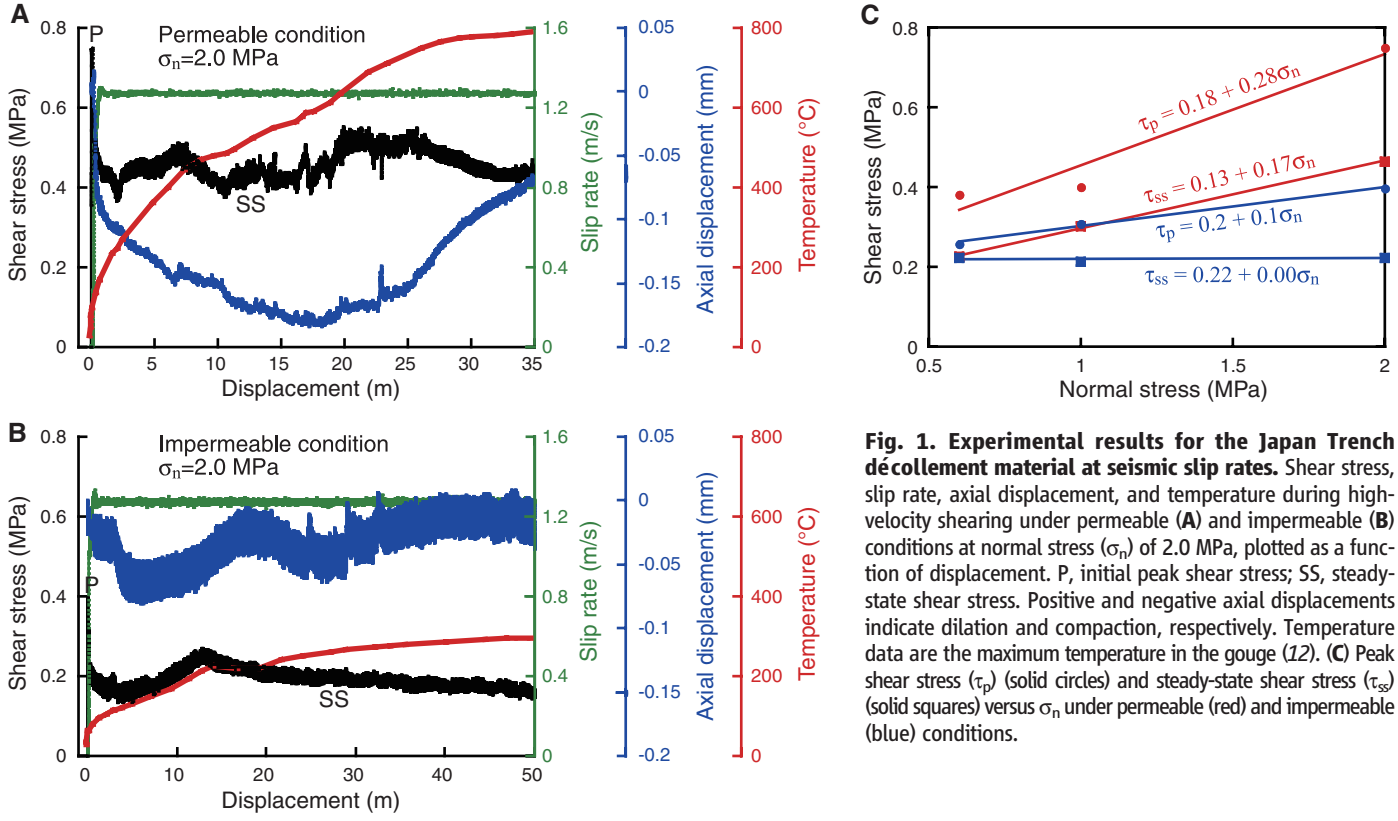

Fig. 1. Experimental results for the Japan Trench décollement material at seismic slip rates. Shear stress, slip rate, axial displacement, and temperature during high-velocity shearing under permeable (**A**) and impermeable (**B**) conditions at normal stress (σ_n) of 2.0 MPa, plotted as a function of displacement. P, initial peak shear stress; SS, steady-state shear stress. Positive and negative axial displacements indicate dilation and compaction, respectively. Temperature data are the maximum temperature in the gouge (*12*). (**C**) Peak shear stress (τ_p) (solid circles) and steady-state shear stress (τ_{ss}) (solid squares) versus σ_n under permeable (red) and impermeable (blue) conditions.

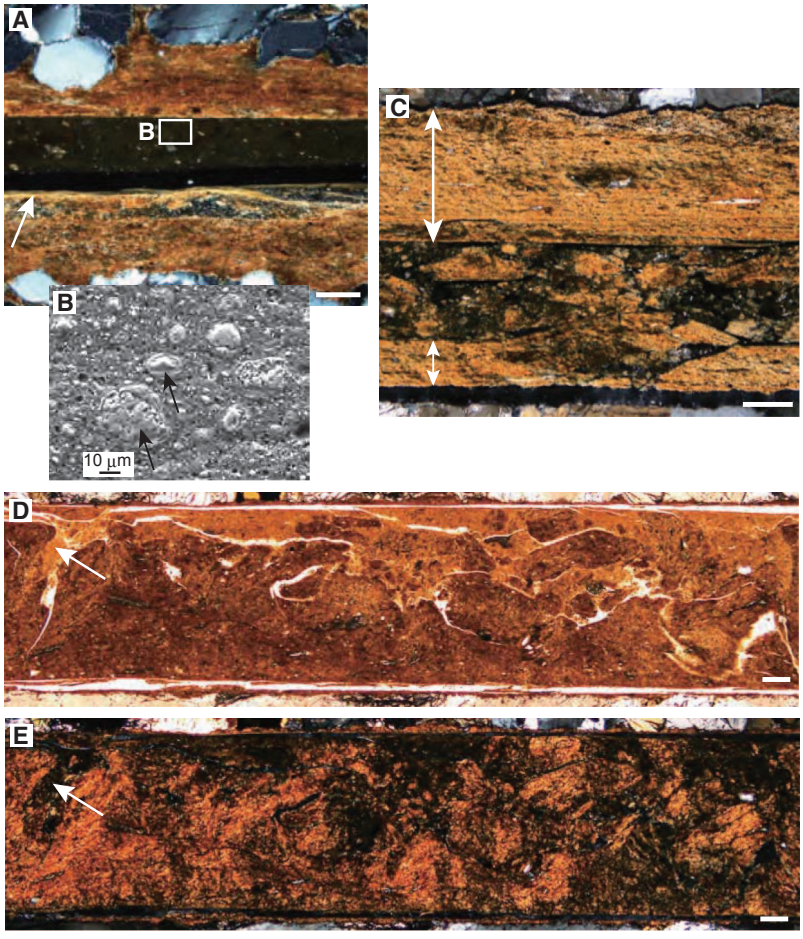

Fig. 2. Microstructures of experimental samples. (**A**) Microstructures after testing under permeable conditions under cross-polarized light. The white arrow indicates the zone of foliated clay. (**B**) Scanning electron microscope back-scattered image showing random orientation of clay-clast aggregates (black arrows) in the matrix. Location of the image is shown in (A). (**C** to **E**) Microstructures after tests under impermeable conditions. (C) Two foliated zones (double white arrows) are apparent in the gouge under cross-polarized light. A portion of the lower foliated zone is just incorporated into the matrix (the middle-lower part of the photograph). (D) Injection structures (white arrow) and fragmentation of clays, suggesting the mobilization of the gouge material due to fluidization, under plane-polarized light. (E) Same as in (D) under cross-polarized light. All microstructural features in this figure are absent in the gouge before high-velocity shearing. White scale bars, 0.1 mm.

the apparent coefficient of friction estimated from the temperature anomaly at the plate-boundary thrust are 0.54 MPa and 0.08, respectively (*17*). Comparisons of these values show that the frictional level estimated from the fault-zone temperature measurements is intermediate between the permeable and impermeable laboratory results on the fault gouge, but closer to the impermeable condition. It is likely that the Tohoku earthquake faulting occurred under only weakly drained or impermeable conditions.

After the experiments, we examined microstructures of the gouge. Thin sections cut tangential to the outer rims of the specimen assembly (2.5 mm from the cylinder boundary and 33 mm from the upper and lower boundaries of the rock specimen) show clay foliations parallel to gouge boundaries and random orientation of fragments in the matrix (Fig. 2). The thickness of the gouge layer before high-velocity shearing is 0.8 mm. Following the permeable experiments, some fragments in the gouge matrix are defined by quartz or feldspar grains surrounded by a cortex of concentric clays (Fig. 2B). These spherical aggregates resemble clay-clast aggregates, which are seen after dry (room humidity) frictional experiments on clay-rich gouges (*18*–*20*). The clay-clast aggregates may form as the water escapes from the gouge during permeable experiments. Following the impermeable experiments, the foliated zones in the gouge are incorporated into the extremely fine-grained matrix in some places (Fig. 2C). In other places, injection of extremely fined-grained material and mixing of materials of different colors without shear surfaces are observed (Fig. 2, D and E). These deformation features and temporal relation of microstructures show that the slip along the foliated zone was followed by fluidization (a phenomenon by which gouge materials in suspension move with a mean free path like that of gas molecules, which is favored by low effective normal stress). The microstructures of the fluidized gouge and the independence of steady-state shear stress on normal stress under the impermeable condition are compelling indications

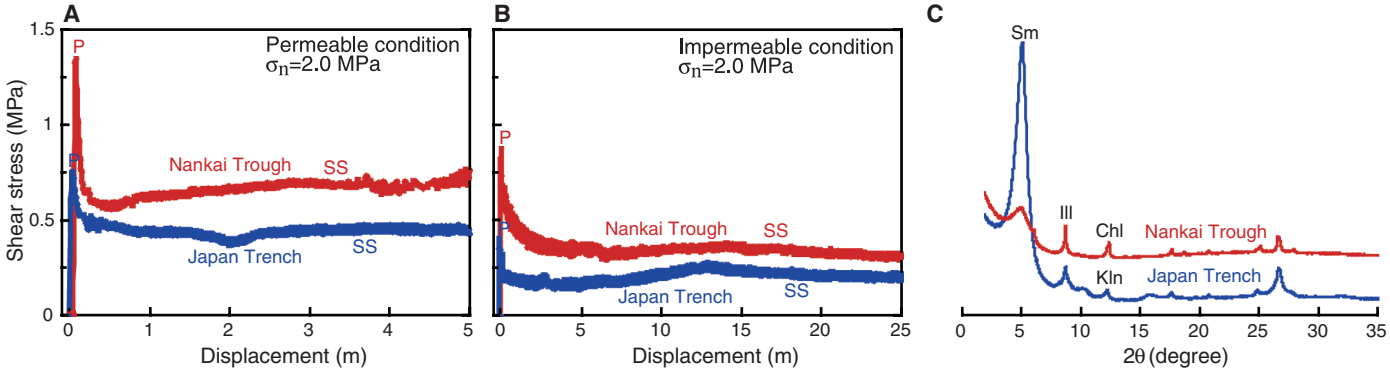

Fig. 3. Comparison of experimental results for décollement materials of the Japan Trench and the Nankai Trough. Shear stress measured during high-velocity shearing under permeable (**A**) and impermeable (**B**) conditions at σ_n of 2.0 MPa, plotted as a function of displacement. P, initial peak shear stress; SS, steady-state shear stress. (**C**) X-ray diffraction patterns for the décollement materials from the Japan Trench and the Nankai Trough, obtained for the <2-μm fractions in the ethylene-glycoled state. Sm, smectite; Ill, illite; Chl, chlorite; Kln, kaolinite.

of thermal pressurization of pore fluid and that the gouge behaved like a fluid during high-velocity shearing.

Our experiments show that the Japan Trench décollement material behaves in a manner that promotes further large displacement once high-velocity slip initiates, predominately due to very low shear stress. To understand if this is similar to the behavior of material from other subduction zones, we also performed high-velocity friction experiments on décollement materials for the Nankai Trough (*12*). Like materials from the Japan Trench, the Nankai Trough materials also exhibit lower shear stress in the experiments under impermeable conditions than in those under permeable conditions, consistent with the idea that low-permeability conditions better contain pore fluid so that thermal pressurization occurs more effectively (Fig. 3, A and B). However, when we compare the data obtained under the same experimental conditions for the two different regions, the décollement material from the Japan Trench has overall lower shear stress from peak to steady-state conditions than the material from the Nankai Trough.

The clay content and clay mineralogy of the fault-zone material differs between the Japan Trench and the Nankai Trough (Fig. 3C) (*12*). The décollement of the Nankai Trough developed in the hemipelagic mudstone (*21*), whereas that of the Japan Trench is localized in pelagic clays (*10*). The total clay content in the Nankai décollement is estimated to be 65% (*21*), compared with 85% for the Japan Trench décollement. The smectite content in the Nankai Trough and Japan Trench décollements is 31 and 78% of the total mineralogy, respectively (*12*). Smectite is known as one of the lowest-friction minerals (*22*, *23*). The abundance of smectite means that large slip on the shallow plate-boundary thrust of the Japan Trench can occur more easily than for the Nankai Trough.

Our results indicate that large slip resulted from coseismic weakening of the fault due to the abundance of smectite and thermal pressurization. Seismic slip could be promoted even in unstrained portions at shallow depths, as the slip propagates through the smectite-rich fault material under fluid-saturated, impermeable conditions. Similar pelagic clay is widely distributed on the ocean floor, and plate-boundary décollements have developed in these smectite-rich sediment layers at several subduction zones (*24*, *25*). Such regions also have the potential for very large coseismic displacements on shallow faults, which could generate very large tsunamis similar to the 2011 Tohoku-Oki earthquake.

References and Notes

1. S. L. Bilek, T. Lay, *Geophys. Res. Lett.* **29**, 18-1–18-4 (2002).
2. J. C. Moore, D. Saffer, *Geology* **29**, 183–186 (2001).
3. K. Wang, Y. Hu, *J. Geophys. Res.* **111**, B06410 (2006).
4. S. Ide, A. Baltay, G. C. Beroza, *Science* **332**, 1426–1429 (2011).
5. Y. Ito *et al.*, *Geophys. Res. Lett.* **38**, L00G05 (2011).
6. T. Fujiwara *et al.*, *Science* **334**, 1240 (2011).
7. S. Kodaira *et al.*, *Nat. Geosci.* **5**, 646–650 (2012).
8. Y. Fujii, K. Satake, S. Sakai, M. Shinohara, T. Kanazawa, *Earth Planets Space* **63**, 815–820 (2011).
9. J. Mori, F. M. Chester, N. Eguchi, S. Toczko, *IODP Sci. Prosp.* 343 10.2204/iodp.sp.343.2012 (2012).
10. F. M. Chester *et al.*, *Science* **342**, 1208–1211 (2013).
11. Shipboard Scientific Party, Site 436: Japan Trench outer rise, Leg 56. Vol. 56, 57 (Pt. 1) (1980).
12. Material and methods are available as supplementary materials on *Science* Online.
13. B. J. Skinner, *Geol. Soc. Am.* **97**, 75–96 (1966).
14. R. H. Sibson, *Nature* **243**, 66–68 (1973).
15. C. W. Mase, L. Smith, *J. Geophys. Res.* **92**, 6249–6272 (1987).
16. J. R. Rice, *J. Geophys. Res.* **111**, B05311 (2006).
17. P. M. Fulton *et al.*, *Science* **342**, 1214–1217 (2013).
18. S. Boutareaud *et al.*, *Geophys. Res. Lett.* **35**, L05302 (2008).
19. K. Ujiie, A. Tsutsumi, *Geophys. Res. Lett.* **37**, L24310 (2010).
20. F. Ferri *et al.*, *J. Geophys. Res.* **116**, B09208 (2011).
21. M. Kinoshita *et al.*, in *Proceedings of the Integrated Ocean Drilling Program* (IODP, Tokyo, 2009), vol. 314/315/316; 10.2204/iodp.proc.314315316.133.2009.
22. J. D. Byerlee, *Pure Appl. Geophys.* **116**, 615–626 (1978).
23. M. J. Ikari, D. M. Saffer, C. Marone, *J. Geophys. Res.* **114**, B05409 (2009).
24. A. Maltman, P. Labaume, B. Housen, *Proc. Ocean Drill. Program Sci. Rep.* **156**, 279–292 (1997).
25. H. Tobin, P. Vannucchi, M. Meschede, *Geology* **29**, 907–910 (2001).

Acknowledgments: For this research, we used samples and data provided by the IODP (www.iodp.org/access-data-and-samples). We thank all drilling and logging operation staff on board the *D/V Chikyu* during Expedition 343 and 343T. We acknowledge two anonymous reviewers for their thoughtful reviews. Part of this work was supported by the U.S. Science Support Program of IODP. K.U. was supported by grant 21107005 (Ministry of Education, Culture, Sports, Science and Technology of Japan). E.E.B was supported by the Gordon and Betty Moore Foundation.

Supplementary Materials

www.sciencemag.org/content/342/6163/1211/suppl/DC1
Materials and Methods
Supplementary Text
Figs. S1 to S5
Tables S1 and S2
References (*26*–*30*)

19 July 2013; accepted 30 October 2013
10.1126/science.1243485

Low Coseismic Friction on the Tohoku-Oki Fault Determined from Temperature Measurements

P. M. Fulton,[1]* E. E. Brodsky,[1] Y. Kano,[2] J. Mori,[2] F. Chester,[3] T. Ishikawa,[4] R. N. Harris,[5] W. Lin,[4] N. Eguchi,[6] S. Toczko,[6] Expedition 343, 343T, and KR13-08 Scientists†

The frictional resistance on a fault during slip controls earthquake dynamics. Friction dissipates heat during an earthquake; therefore, the fault temperature after an earthquake provides insight into the level of friction. The Japan Trench Fast Drilling Project (Integrated Ocean Drilling Program Expedition 343 and 343T) installed a borehole temperature observatory 16 months after the March 2011 moment magnitude 9.0 Tohoku-Oki earthquake across the fault where slip was ~50 meters near the trench. After 9 months of operation, the complete sensor string was recovered. A 0.31°C temperature anomaly at the plate boundary fault corresponds to 27 megajoules per square meter of dissipated energy during the earthquake. The resulting apparent friction coefficient of 0.08 is considerably smaller than static values for most rocks.

Earthquake rupture propagation and slip are moderated by the dynamic shear resistance on the fault. Any complete model of earthquake growth therefore requires quantification of shear stress, which is difficult to measure. Historically, the shear stress during an earthquake was thought to nearly equal that controlled by static friction, but recent laboratory experiments and field observations have brought this assumption into question (*1*, *2*). Direct measurement of the magnitude of earthquake stress is challenging because seismological measurements only record stress changes.

Rapid-response drilling provides a solution (*3*). Because the frictional stress during slip results in dissipated heat, subsurface temperature measurements soon after a major earthquake can record the temperature increase over the fault and its decay. If the slip on the fault is known, the thermal observations allow one to infer the frictional shear stress (*4*, *5*). On 15 July 2012, as part of the Japan Trench Fast Drilling Project (JFAST) [Integrated Ocean Drilling Program (IODP) Expedition 343 and 343T], we installed a sub–sea-floor temperature observatory in the

[1]Department of Earth and Planetary Sciences, University of California, Santa Cruz, CA, USA. [2]Disaster Prevention Research Institute, Kyoto University, Kyoto, Japan. [3]Center for Tectonophysics, Department of Geology and Geophysics, Texas A&M University, College Station, TX, USA. [4]Kochi Institute for Core Sample Research, Japan Agency for Marine-Earth Science and Technology, Kochi, Japan. [5]Oregon State University, Corvallis, OR, USA. [6]Center for Deep Earth Exploration, Japan Agency for Marine-Earth Science and Technology, Yokohama, Japan.

*Corresponding author. E-mail: pfulton@ucsc.edu
†Expedition 343, 343T, and KR13-08 Scientists authors and affiliations are listed in the supplementary materials.

Low Coseismic Shear Stress on the Tohoku-Oki Megathrust Determined from Laboratory Experiments

Kohtaro Ujiie, Hanae Tanaka, Tsubasa Saito, Akito Tsutsumi, James J. Mori, Jun Kameda, Emily E. Brodsky, Frederick M. Chester, Nobuhisa Eguchi, Sean Toczko and Expedition 343 and 343T Scientists

Science **342** (6163), 1211-1214.
DOI: 10.1126/science.1243485

Deep Drilling for Earthquake Clues

The 2011 M_W 9.0 Tohoku-Oki earthquake and tsunami were remarkable in many regards, including the rupturing of shallow trench sediments with huge associated slip (see the Perspective by **Wang and Kinoshita**). The Japan Trench Fast Drilling Project rapid response drilling expedition sought to sample and monitor the fault zone directly through a series of boreholes. **Chester *et al.*** (p. 1208) describe the structure and composition of the thin fault zone, which is predominately comprised of weak clay-rich sediments. Using these same fault-zone materials, **Ujiie *et al.*** (p. 1211) performed high-velocity frictional experiments to determine the physical controls on the large slip that occurred during the earthquake. Finally, **Fulton *et al.*** (p. 1214) measured in situ temperature anomalies across the fault zone for 9 months, establishing a baseline for frictional resistance and stress during and following the earthquake.